JOURNAL OF APPLIED PHYSICS **119**, 145705 (2016)

The fine structure of electron irradiation induced EL2-like defects in *n*-GaAs

S. M. Tunhuma, F. D. Auret, M. J. Legodi, and M. Diale
Department of Physics, University of Pretoria, Private Bag X20, Pretoria 0002, South Africa

(Received 11 February 2016; accepted 29 March 2016; published online 13 April 2016)

Defects induced by electron irradiation in *n*-GaAs have been studied using deep level transient spectroscopy (DLTS) and Laplace DLTS (L-DLTS). The $E_{0.83}$ (EL2) is the only defect observed prior to irradiation. Ru/*n*-GaAs Schottky diodes were irradiated with high energy electrons from a Sr-90 radionuclide up to a fluence of $2.45 \times 10^{13}\,cm^{-2}$. The prominent electron irradiation induced defects, $E_{0.04}$, $E_{0.14}$, $E_{0.38}$, and $E_{0.63}$, were observed together with the metastable $E_{0.17}$. Using L-DLTS, we observed the fine structure of a broad base EL2-like defect peak. This was found to be made up of the $E_{0.75}$, $E_{0.83}$, and $E_{0.85}$ defects. Our study reveals that high energy electron irradiation increases the concentration of the $E_{0.83}$ defect and introduces a family of defects with electronic properties similar to those of the EL2. © *2016 AIP Publishing LLC*. [http://dx.doi.org/10.1063/1.4945774]

I. INTRODUCTION

Defect engineering has enabled the development of optimized semiconductor material structures. In some semiconductor materials, point defect engineering has improved device performance and suppressed undesirable properties.[1,2] Particle irradiation induced defects modify the electronic properties of semiconductors.[3] These modifications lead to applications such as carrier lifetime control and device isolation.[4] Understanding the physical properties and occurrence of defects will potentially lead to improved device designs.

In the past, studies have been carried out to gain insight into defects induced by particle irradiation on GaAs devices.[5,6] Such information is vital considering the wide range of optoelectronic applications of these devices under various conditions. An example of such an application is the use of GaAs solar cells in space where they are exposed to highly energetic radiation particles.[7] Moreover, in developing future technologies, for both natural and harsh radiation environments, it is crucial to have a clear view of potential radiation problems.

The EL2 defect is very important in GaAs because it affects the optical properties and controls the performance of GaAs based devices.[8,9] In some instances, the defect traps electrons when they are accelerated into semi-insulating regions and may create regions of fixed trap charge that can ruin devices.[10] On the other hand, it can be deliberately introduced to increase resistivity of bulk GaAs so as to lower substrate capacitance and allow high frequency operation of devices. It is arguably the most studied defect in semiconductor physics, with a lot of controversy among researchers for many years, concerning its properties and microscopic structure.[11–14] All the microscopic models that exist are only coherent in that the properties of the EL2 are As antisite related.[15] An alternate viewpoint proposes oxygen related centers.[16] It has also been postulated that there exists a whole family of midgap levels so called the "EL2 family."

The limitation in most of these studies was the low resolution of conventional deep level transient spectroscopy (DLTS). DLTS is a technique for studying defects in semiconductors, which displays emission data spectroscopically as a function of temperature.[17] Conventional DLTS is unable to distinguish defects that have similar energies within the bandgap, which are shown as single, broad based peaks.[18] As a result, most reports on induced defects in n-GaAs have not reported on the fine structure of the defects. L-DLTS provides a solution by offering up to an order of magnitude increase in resolution.[18,19] Dobaczewski *et al.*[20] were the first to use L-DLTS to study the EL2 in GaAs. They did a comparative study of five liquid encapsulated Czokralski (LEC) grown GaAs crystals from different sources and they observed a defect family of at least two peaks in each sample.

This work adds on to this body of knowledge, by considering MOVPE grown *n*-GaAs. We have investigated the defects introduced in Ru/*n*-GaAs Schottky barrier diodes by electron irradiation using DLTS. Using L-DLTS, we explored the fine structure and annealing behavior of these defects in detail for the first time. The results show two EL2-like midgap energy levels. In the nomenclature used in this article, we shall refer to them as radiation induced (RI) EL2-like defects. This is an important result especially considering the interest in defect engineering using the EL2 and recent progress in growth of cheaper GaAs which is going to be highly influenced by the presence of defects in the material.[10,21]

II. EXPERIMENTAL PROCEDURE

Si doped *n*-GaAs (1 0 0) epitaxial layers (5 μm) grown by MOVPE on n^+ GaAs substrates were used in this study. The average free carrier density was $1.0 \times 10^{15}\,cm^{-3}$ as specified by the suppliers (Spire Corporation). First, the samples were degreased and etched chemically. An Au:Ge (88%:12%) eutectic was thermally evaporated in a resistive deposition system on the n^+ sides to form an ohmic contact, with an Au overlayer. This was followed by a 2 min anneal in Ar at 450 °C. Thereafter, 1000 Å thick Ru contacts, 0.6 mm in diameter, were deposited on the epitaxial layer using electron beam evaporation. Contact quality was evaluated using current-voltage (*I-V*) and capacitance-voltage (*C-V*) measurements.

The devices were then irradiated with MeV electrons for 5 h up to a dose of $2.45 \times 10^{13}\,cm^{-2}$ from a Sr-90

radionuclide. A detailed graphical representation of the energy distribution of electrons emitted by the radionuclide is given by Auret *et al.*[22] The carrier concentration of the samples after irradiation was monitored through *C-V* measurements in order to see whether the accuracy of the DLTS measurements was not being compromised by a high radiation dose through carrier removal. DLTS spectra were recorded at a scan rate of 2 K/min in the 15–390 K temperature range, at a quiescent reverse bias (V_R) of −2 V, filling pulse amplitude (V_p) −0.2 V, and filling pulse width (t_p) 1 ms. The defects observed from the scans were characterized using L-DLTS.[20] The forward bias filling pulse was set at −0.2 V in order to avoid the capacitance signal from surface states. Surface states are sometimes confused with, or prevent, the detection of deep levels in the bulk of the material.[23,24]

The signatures (energy level in the band gap (E_t), and apparent capture cross section (σ_n)) of the induced defects were calculated using log (e_n/T^2) versus (1000/T) Arrhenius plots, from the slope and y-intercept, respectively, according to the following equation:[18]

$$e_n = \sigma_n \langle v_{th} \rangle \frac{g_o}{g_1} N_c \exp\left(-\frac{E_c - E_t}{k_B T}\right). \quad (1)$$

Equation (1) gives the emission rate as a function of temperature T, where $\langle v_{th} \rangle$ is the thermal velocity of electrons, $(E_c - E_t)$ is the activation energy, N_c is the density of conduction band states, g_0 and g_1 are the degeneracy terms referring to the states before and after electron emission, and k_B is the Boltzmann constant. Capture cross section is assumed to have a T^2 dependency, hence the log(e_n/T^2) versus 1000/T plots. The true capture cross section of some of the defects was then obtained using the pulse width method, which is described briefly in Sec. III B. In-order to investigate the thermal stability of the defects, the samples were annealed in the 0–300 °C range with incremental steps of 50 °C.

III. RESULTS AND DISCUSSION

A. Electron irradiation induced defects

Irradiation induced defects emanate from collisions of energetic particles which results in elastic scattering. The Frenkel pair is created when a particle imparts energy to a lattice atom to displace it forming a vacancy-interstitial pair. Mobile vacancies and interstitials are also introduced through the same mechanism. At room temperature, the threshold displacement energy in GaAs has been observed to be approximately 9.0 eV in Ga and approximately 9.4 eV in As.[25]

Figure 1 depicts the results of the DLTS scans obtained at a rate window of 4 Hz. Curve (a) is the control spectrum obtained from the as-deposited samples before irradiation. It shows only the native ($E_{0.83}$) defect present, which is also well known as the EL2 defect. Similarly, the 0.83 eV energy level has been observed in GaAs (as-grown) samples by other researchers and in GaAs based structures grown through molecular beam epitaxy and LEC.[17,26–28] The EL2 defect can exist in two different atomic configurations, a normal configuration and a metastable one. The metastable

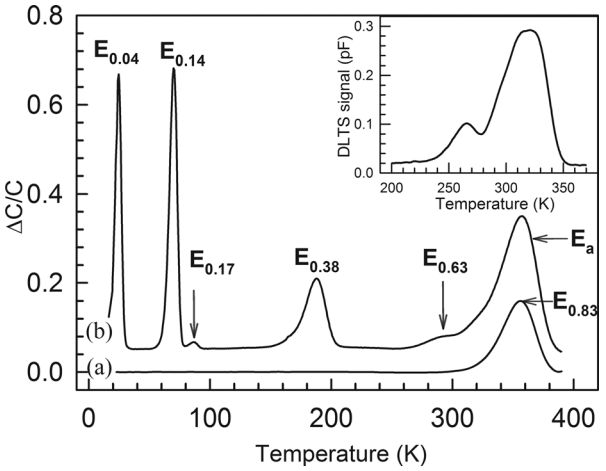

FIG. 1. DLTS spectra of (a) as grown samples. (b) MeV electron irradiated samples recorded at a quiescent reverse bias (V_R) of −2 V at a rate window of 4 Hz, filling pulse (V_p) of −0.2 V, and pulse width (t_p) of 1 ms. E_a is a compound peak of three defects. Inset: Broad peaks observed after radiation exposure for 24 h.

configuration is attainable by photoquenching at low temperatures in which all the optical, magnetic, and electrical properties disappear.[29]

Dobaczewski *et al.*[17] reported the presence of four energy levels associated with the EL2 in LEC as-grown samples measured by L-DLTS. In our as grown samples, only the $E_{0.83}$ was observed in a measurable concentration before irradiation. The presence of As antisite related defects in GaAs is highly dependent on the growth conditions, namely, growth rate, stoichiometry, and temperature.[30,31] Curve (b) reveals emission peaks from defects induced by electron irradiation into the GaAs. The peaks have been labeled $E_{0.04}$, $E_{0.14}$, $E_{0.17}$, $E_{0.38}$, and $E_{0.63}$ based on their energy levels. Additionally, a compound broad based peak has been labeled E_a.

A metastable defect that has been reported, in the same temperature range, superimposed on the $E_{0.38}$ peak, was not observed in our scans.[32] This is because of its presence, and the magnitude is highly dependent on the bias conditions, temperature-cycling, and incident particle type. The $E_{0.04}$, $E_{0.14}$, and $E_{0.38}$ defects have the same electronic structure and are point defect in nature. They are termed *primary electron irradiation induced defects* as they are observable with the same signatures after being induced by different radiation types.[33] The defects $E_{0.04}$ and $E_{0.14}$ are different charge states of the isolated As vacancy. Also, the $E_{0.38}$ has been attributed to close As vacancy-interstitial pairs, and its behavior is bound to the mobility of the arsenic interstitial after studying the introduction rate versus flux of electron irradiation and thermal annealing.[34,35] The $E_{0.17}$ defect is metastable and can be reversibly transformed by introducing zero and reverse bias anneals.[36] Finally, the $E_{0.63}$ can only be observed at relatively high radiation fluencies which implies that it might be a complex defect.

B. The fine structure of the radiation induced EL2-like defects

Using L-DLTS, we were able to resolve the fine structure of the broad peak labeled E_a in Figure 1. As a result,

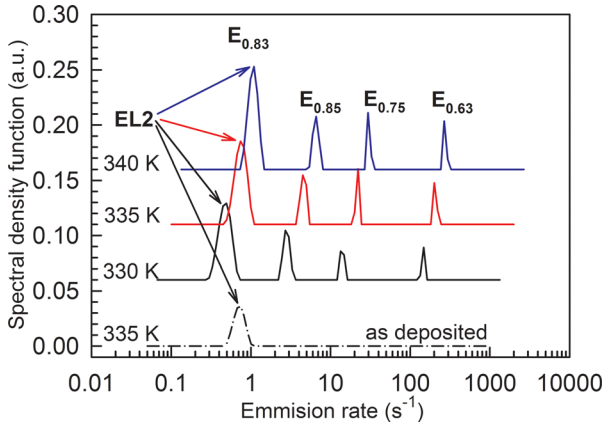

FIG. 2. Laplace DLTS spectra showing the EL2 and radiation induced EL2-like defects in MOVPE grown *n*-GaAs and the reference spectrum.

three unique energy levels were identified which are displayed in Figure 2 as $E_{0.75}$, $E_{0.83}$, and $E_{0.85}$, respectively. The $E_{0.63}$ already appears on the DLTS spectrum (b) in Figure 1. By varying pulse width and observing the spectral response, we confirmed that we were probing different and unique energy states. The Arrhenius plots of the three energy levels with the $E_{0.63}$ are shown in Figure 3. In general, several authors have reported on the existence of least two midgap energy levels in n-GaAs. Dobaczewski *et al.*[17] reported four energy levels similar to Figure 2 in LEC (as-grown) samples using Laplace DLTS. Saxena[37] observed the 0.76 eV and 0.83 eV energy levels using capacitance-voltage-time measurements. Furthermore, similar energy levels to those found in our experiments have been reported by other researchers. The 0.75 eV has been observed in InAs quantum dots embedded in a GaAs matrix using L-DLTS,[27] and the 0.85 eV energy level was predicted by Li *et al.*,[38] using density functional theory (DFT) calculations on supercells of 64 atoms. Hall Effect measurements on the EL2 have determined the energy range to be in the 0.72 eV to 0.80 eV range.[39] However, Bourgoin *et al.*[46] gave a detailed account on why Hall measurement results cannot reliably measure the energy level of the EL2. Arrhenius plots of all the defects identified in this study are shown in Figure 4. The resulting defect

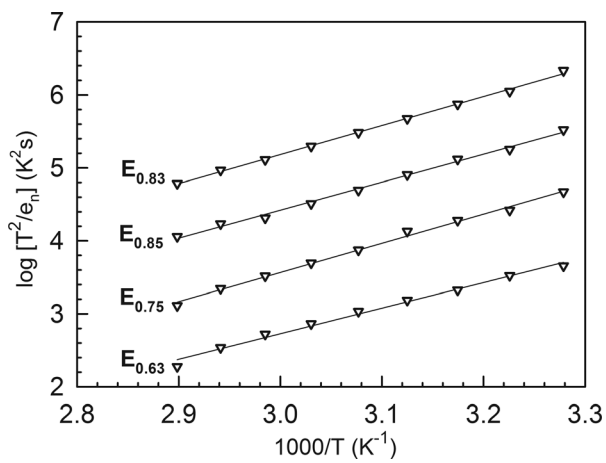

FIG. 3. Arrhenius plots for the EL2 and EL2-like electron irradiation induced defects.

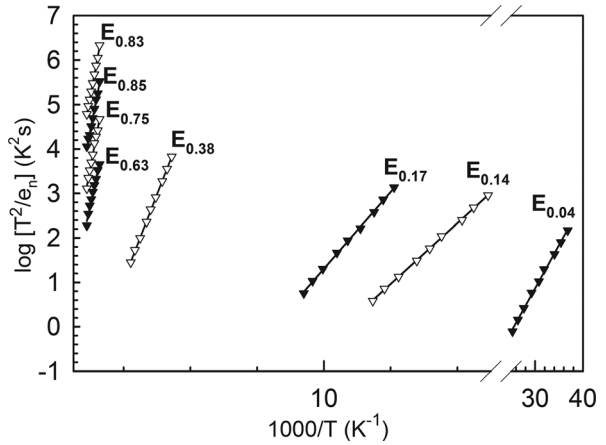

FIG. 4. Arrhenius plots for defects introduced by MeV electrons in MOVPE grown *n*-GaAs.

"signatures" are summarized in Table I. Apparent capture cross section calculations obtained directly from Equation (1) have been shown in the past to be erroneous since in some instances they do not account for temperature and electric field dependencies.[40] The accurate capture cross section values can be obtained by using the filling pulse, a technique which is highly demanding in terms of instrumentation.[41] In principle, trap filling will proceed exponentially with a time constant given by the following equation:[42]

$$\tau_c = \frac{1}{\sigma_n v_{th} n}, \tag{2}$$

where n is the free carrier concentration at the measurement temperature. By monitoring the peak of the DLTS signal as a function of filling pulse as shown in Figure 5, we determined τ_c from the slopes of the semi-logarithmic graphs. The results are displayed in Table II showing an almost similar σ_n for the $E_{0.83}$ and $E_{0.85}$ and a lower value by almost two orders of magnitude for the $E_{0.75}$.

Spatial distribution of the electron irradiation induced defects in GaAs was obtained using the fixed bias, variable pulse method.[43] Profiling of the depth distribution of the defects was done at a constant reverse bias of −5 V. Additionally, a comparison was done between the concentration depth of the $E_{0.83}$ before and after irradiation as displayed in Figure 6. The defect concentration of the $E_{0.83}$ shows a general decrease deeper into the bulk. A comparison

TABLE I. Electronic properties of defects in MeV electron irradiated, MOVPE grown *n*-GaAs obtained by Arrhenius analysis at $V_R = -2.0$ V, $V_P = -0.2$ V, and $t_p = 1$ ms.

Defect label	E_t (meV)	σ_n (cm^{-2})
$E_{0.04}$	38.7	1.6×10^{-17}
$E_{0.14}$	135	3.0×10^{-15}
$E_{0.17}$	171	3.4×10^{-13}
$E_{0.38}$	382	7.4×10^{-16}
$E_{0.63}$	634	1.0×10^{-15}
$E_{0.75}$	749	5.2×10^{-15}
$E_{0.83}$ (EL2)	833	2.8×10^{-15}
$E_{0.85}$	852	3.4×10^{-14}

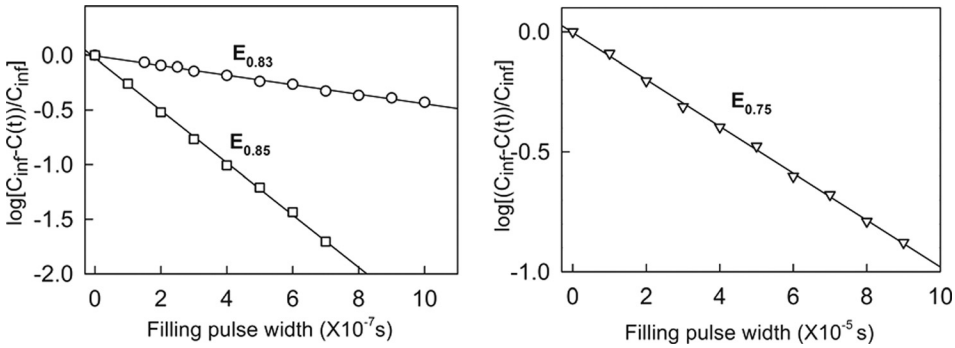

FIG. 5. Determination of accurate capture cross section of the EL2 radiation induced EL2-like defects using the pulse width method at 320 K.

TABLE II. Values of the capture time constant (τ) and capture cross section (σ_n) for defects in the EL2-like defects obtained using the pulse width method at 320 K.

Defect label	τ(s)	σ_n(cm$^{-2)}$
$E_{0.75}$	4.2×10^{-7}	5.5×10^{-15}
$E_{0.83}$ (EL2)	2.3×10^{-6}	1.0×10^{-15}
$E_{0.85}$	1.0×10^{-4}	2.3×10^{-17}

of its depth profiles before and after irradiation shows an increase in the defect concentration of close to an order of magnitude as a result of the electron irradiation. Depth profiles of the $E_{0.85}$ and $E_{0.75}$ defects are similar and flat. The $E_{0.83}$ is at a higher concentration than the rest of the defects, explaining why it is the one most likely to be detected by DLTS measurements. Concentrations of these defects are consistent with the 10^{16} to 10^{13} cm^{-3} range that was reported for EL2 defects by other researchers in VPE grown n-GaAs.[44]

C. Annealing of the EL2-like radiation-induced defects

In our previous study, we investigated the effect of dynamic annealing on the electrical characteristics of Au/*n*-GaAs Schottky barrier diodes.[45] We attributed an inconsistency in the behavioral trend of the *C-V* barrier height to the EL2 defect. Figure 7 shows the results of our measurements on the thermal stability of the radiation induced EL2-like

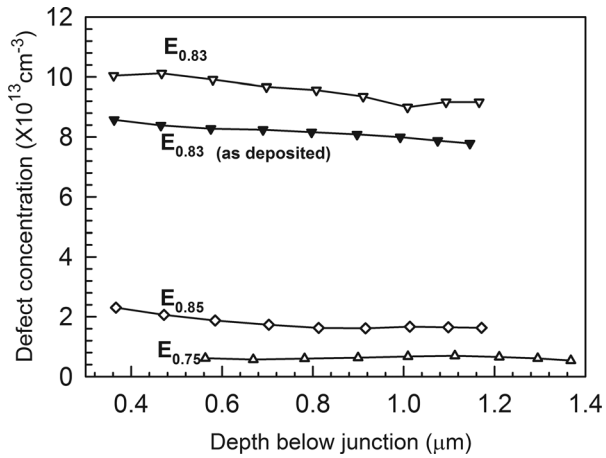

FIG. 6. Depth and concentration of the defects introduced by MeV electrons in Ru/*n*-GaAs Schottky diodes compared to as deposited (unirradiated) samples.

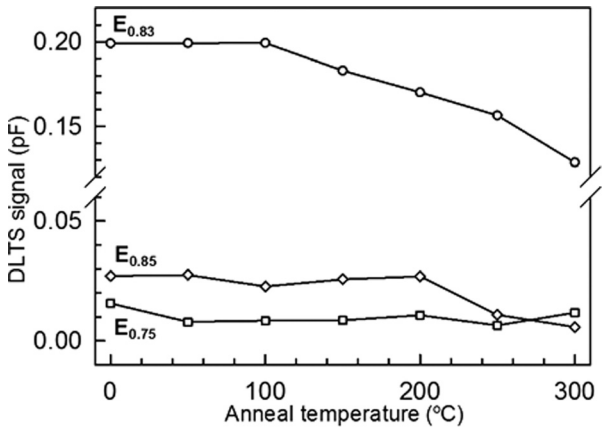

FIG. 7. Isochronal annealing (5 min periods) of the EL2 and radiation induced EL2-like defects in *n*-GaAs.

defects on Ru/*n*-GaAs Schottky barrier diodes. It was only after annealing at 100 °C there was a notable decrease in the concentration of the $E_{0.83}$. Its overall reduction in concentration after annealing at 300 °C was 65%, whereas that for the $E_{0.85}$ was 21% when compared to unannealed samples. An inconsistent trend was observed for the $E_{0.75}$ throughout the annealing steps. The overall difference in behavior during annealing suggests that all radiation induced EL2-like defects might be of different species. Also, the annealing behavior of the EL2 in this case suggests carrier removal, which is consistent with our findings in Ref. 45.

IV. CONCLUSIONS

Ru Schottky barrier diodes were fabricated on *n*-type GaAs. DLTS measurements were carried out before and after high energy electron irradiation. The $E_{0.04}$, $E_{0.14}$, $E_{0.17}$, $E_{0.38}$, $E_{0.63}$, $E_{0.75}$, and $E_{0.85}$ defects were detected after irradiation. Irradiation increased the defect concentration of the native $E_{0.83}$ defect found in as deposited samples. Performing L-DLTS on the broad EL2-like peak revealed the $E_{0.75}$, $E_{0.85}$, and $E_{0.83}$ defects. Using the pulse width method, the accurate capture cross section of the EL2 and EL2-like defects was measured. The true capture cross sections for the $E_{0.83}$ and $E_{0.85}$ were observed to be almost similar and greater than those for the $E_{0.75}$ by almost two orders of magnitude. Depth profiling was also done using the fixed bias variable pulse method, which showed the higher concentration of the $E_{0.83}$ compared to all the observed defects. Annealing within the 0–300 °C range did not introduce any new defects but led to

the general decrease in concentration of the $E_{0.85}$, $E_{0.83}$, and $E_{0.75}$. We can conclude that in addition to vacancies and interstitials, high energy electron irradiation also induces midgap electron traps with electronic properties similar to the EL2 defects in *n*-GaAs.

ACKNOWLEDGMENTS

The authors gratefully acknowledge the financial support of the South African National Research Foundation (NRF) and the University of Pretoria. Opinions, findings, and conclusions expressed in this publication are those of the authors and the NRF accepts no liability. The Laplace DLTS system used in the research was kindly provided by A. R. Peaker (Center for Electronic Materials Devices and Nanostructures, University of Manchester) and L. Dobaczewski (Institute of Physics, Polish Academy of Sciences).

[1]L. Hu, T. Zhu, X. Liu, and X. Zhao, Adv. Funct. Mater. **24**, 5211 (2014).
[2]A. Chroneos, C. A. Londos, E. N. Sgourou, and P. Pochet, Appl. Phys. Lett. **99**, 241901 (2011).
[3]E. Omotoso, W. E. Meyer, F. D. Auret, A. T. Paradzah, M. Diale, S. M. M. Coelho, and P. J. Janse van Rensburg, Mater. Sci. Semicond. Process. **39**, 112 (2015).
[4]W. E. Meyer, F. D. Auret, and S. A. Goodman, Jpn. J. Appl. Phys. Lett. **35**, L1 (1996).
[5]M. J. Legodi, F. D. Auret, and S. A. Goodman, Physica B: Condens. Matter **273–274**, 762 (1999).
[6]D. Pons and J. C. Bourgoin, J. Phys. C: Solid State Phys. **18**, 3839 (1985).
[7]M. Yamaguchi, Y. Ohmachi, T. Oh'hara, Y. Kadota, M. Imaizumi, and S. Matsuda, Prog. Photovoltaics: Res. Appl. **9**, 191 (2001).
[8]W. Shi, R. Liu, and J. L. Wang, "Effects of EL2 deep level in GaAs photoconductive switch," in *Proceedings SPIE 7385, International Symposium on Photoelectronic Detection and Imaging 2009: Terahertz and High Energy Radiation Detection Technologies and Applications*, **7385**, 73851R (2009).
[9]T. Kitamoto, Y. Inoue, M. Yamada, and T. Ktawase, Phys. Status Solidi A **204**, 1002 (2007).
[10]A. G. Baca, C. I. H. Ashby, and I. O. E. Engineers, *Fabrication of GaAs Devices* (Institution of Engineering and Technology, 2005).
[11]I. Tkach, K. Krambrock, H. Overhof, and J. M. Spaeth, Physica B: Condens. Matter **340–342**, 353 (2003).
[12]D. Ma, X. Chen, H. Qiao, W. Shi, and E. Li, J. Alloys Compd. **637**, 16 (2015).
[13]M. Kaminska, Phys. Scr. **1987**, 551.
[14]Y. Oyama, H. Dezaki, Y. Shimizu, and K. Maeda, Appl. Phys. Lett. **106**, 022109 (2015).
[15]H. Boudinov, A. V. P. Coelho, H. H. Tan, and C. Jagadish, J. Appl. Phys. **93**, 3234 (2003).
[16]T. Ikoma, M. Taniguchi, and Y. Mochizuki, Microelectron. Eng. **2**, 137 (1984).
[17]L. Dobaczewski, P. Kaczor, I. D. Hawkins, and A. R. Peaker, J. Appl. Phys. **76**, 194 (1994).
[18]A. R. Peaker, V. P. Markevich, I. D. Hawkins, B. Hamilton, K. B. Nielsen, and K. Gościński, Physica B: Condens. Matter **407**, 3026 (2012).
[19]C.-C. Tin, *Characterization of Materials* (John Wiley & Sons, Inc., 2002).
[20]L. Dobaczewski, A. R. Peaker, and K. B. Nielsen, J. Appl. Phys. **96**, 4689 (2004).
[21]G. J. Hayes and B. M. Clemens, MRS Commun. **5**, 1 (2015).
[22]F. D. Auret, S. A. Goodman, G. Myburg, and W. E. Meyer, Appl. Phys. A **56**, 547 (1993).
[23]M. Aziz, P. Ferrandis, A. Mesli, R. Hussain Mari, J. Francisco Felix, A. Sellai, D. Jameel, N. Al Saqri, A. Khatab, D. Taylor, and M. Henini, J. Appl. Phys. **114**, 134507 (2013).
[24]M. Nel and F. D. Auret, J. Appl. Phys. **64**, 2422 (1988).
[25]J. H. Crawford and L. M. Slifkin, *Point Defects in Solids: General and Ionic Crystals* (Springer, USA, 2013).
[26]N. A. Naz, U. S. Qurashi, A. Majid, and M. Z. Iqbal, Physica B: Condens. Matter **404**, 4956 (2009).
[27]W. H. Strong, D. V. Forbes, and S. M. Hubbard, Mater. Sci. Semicond. Process. **25**, 76 (2014).
[28]M. Kaniewska, O. Engström, A. Barcz, and M. Pacholak-Cybulska, Mater. Sci. Eng.: C **26**, 871 (2006).
[29]D. Kabiraj and S. Ghosh, Appl. Phys. Lett. **87**, 252118 (2005).
[30]J. C. Bourgoin, H. Hammadi, M. Stellmacher, J. Nagle, B. Grandidier, D. Stievenard, J. P. Nys, C. Delerue, and M. Lannoo, Physica B: Condens. Matter **273–274**, 725 (1999).
[31]D. B. Holt and B. G. Yacobi, *Extended Defects in Semiconductors: Electronic Properties, Device Effects and Structures* (Cambridge University Press, 2007).
[32]F. D. Auret, S. A. Goodman, and W. E. Meyer, Appl. Phys. Lett. **67**, 3277 (1995).
[33]S. M. Tunhuma, M. J. Legodi, M. Diale, and F. D. Auret, in Proceedings of the SAIP (2015).
[34]D. Stievenard, X. Boddaert, J. C. Bourgoin, and H. J. von Bardeleben, Phys. Rev. B **41**, 5271 (1990).
[35]F. D. Auret, S. A. Goodman, M. Hayes, G. Myburg, W. O. Barnard, and W. E. Meyer, *Electrical Characterization of Particle Induced Damage in n-GaAs*, Vol. 16 (South African Journal of Physics, 1993).
[36]F. D. Auret, M. E. Rudolph, and A. G. Stewart, Jpn. J. Appl. Phys. **33**, L491 (1994).
[37]A. K. Saxena, Physica Status Solidi A **183**, 281 (2001).
[38]D. Li, M. Yang, Y. Cai, S. Zhao, and Y. Feng, Opt. Express **20**, 6258 (2012).
[39]M. Kaminska and E. R. Weber, "EL2 defect in GaAs," in *Semiconductors & Semimetals* (Elsevier Science, 1993).
[40]D. V. Lang, H. G. Grimmeiss, E. Meijer, and M. Jaros, Phys. Rev. B **22**, 3917 (1980).
[41]M. Razeghi, *The MOCVD Challenge: A survey of GaInAsP-InP and GaInAsP-GaAs for Photonic and Electronic Device Applications*, 2nd ed. (CRC Press, 2010).
[42]C. Claeys and E. Simoen, *Radiation Effects in Advanced Semiconductor Materials and Devices* (Springer, Berlin, Heidelberg, 2013).
[43]H. T. Danga, F. D. Auret, S. M. M. Coelho, and M. Diale, Physica B: Condens. Matter **480**, 206–208 (2015).
[44]E. F. Schubert, *Doping in III-V Semiconductors* (Cambridge University Press, 2005).
[45]S. M. Tunhuma, F. D. Auret, M. J. Legodi, and M. Diale, Physica B: Condens. Matter **480**, 201 (2016).
[46]J. C. Bourgoin and T. Neffati, Solid state electronics **43**, 153 (1999).